fit the kinetic data obtained for the CO inhibition of PPh_3 photosubstitution, this intermediate would have to either dissociate CO, an unlikely event for a cluster that is already electron deficient, or competively add CO or PPh_3 to give open $H_2FeRu_3(CO)_{13}L$ clusters, eq 10 and 11. Unimolecular decay of **5** and

$$4 + CO \xrightarrow{k_3} \underset{5}{H_2FeRu_3(CO)_{14}} \quad (10)$$

$$4 + PPh_3 \xrightarrow{k_5} \underset{6}{H_2FeRu_3(CO)_{13}(PPh_3)} \quad (11)$$

6 via CO loss would give $H_2FeRu_3(CO)_{13}$ and $H_2FeRu_3(CO)_{12}(PPh_3)$, respectively, but the net result would be competition of CO with PPh_3 for a common intermediate, and eq 8 would apply. Thus, the kinetic data cannot distinguish between CO dissociation or metal-metal bond cleavage in the primary photochemical event.

However, the lack of significant fragmentation of $H_2FeRu_3(CO)_{13}$ in the presence of CO does argue against metal-metal bond cleavage. An intermediate such as $H_2FeRu_3(CO)_{14}$ formed via reaction 10 is precisely the intermediate whose formation has been implicated in the rate-determining step in the thermal fragmentation of $H_2FeRu_3(CO)_{13}$ with CO.[25] However, this intermediate must decay to fragmentation products very rapidly, since it has never been detected in the thermal reactions. Thus, if this species were formed in the photochemical process, it should decay to fragmentation products and not back to $H_2FeRu_3(CO)_{13}$. Such fragmentation products were not observed and thus metal-metal bond cleavage is not implicated as the *dominant* photoreaction. Also arguing against metal-metal bond cleavage is the lack of PPh_3 concentration dependence on the quantum yield of PPh_3 photosubstitution. If photolysis were to induce metal-metal bond rupture to give an open "butterfly" cluster such as **4** in eq 9, this latter species could decay either by closure to reform the original $H_2FeRu_3(CO)_{13}$ cluster or add PPh_3 followed by CO loss to affect substitution. The relative efficiency of the latter reaction, and hence its quantum yield, would be expected to increase with increasing PPh_3 concentration. Such was not observed, Table II, and metal-metal bond cleavage as the dominant primary photoreaction is not supported. Metal-metal bond cleavage must occur some fraction of the time, however, since it is the only means by which the low quantum yield CO-induced fragmentation of the $H_4M_4(CO)_{13}$ clusters can occur.

Acknowledgment. G.L.G. gratefully acknowledges the Camille and Henry Dreyfus Foundation for a Teacher-Scholar Award (1978-1983). This research was supported by the National Science Foundation (CHE-7728387) and by the Standard Oil Company of Ohio.

Supplementary Material Available: A complete derivation of eq 8 (3 pages). Ordering information is given on any current masthead page.

Photochemistry of Surface-Confined Organometallics. Photochemical Release of a Surface-Confined Cobalt Carbonyl Catalyst†

Carol L. Reichel and Mark S. Wrighton*

Contribution from the Department of Chemistry, Massachusetts Institute of Technology, Cambridge, Massachusetts 02139. *Received February 9, 1981. Revised Manuscript Received June 1, 1981*

Abstract: Inorganic oxide surfaces, SiO_2 and Al_2O_3, bearing -OH functionality have been functionalized with $-Co(CO)_4$ by first treating the solids with $(EtO)_3SiH$, Me_2ClSiH, or Cl_3SiH to introduce [S]>SiH functionality followed by reaction with $Co_2(CO)_8$. Derivatized surfaces have been characterized by infrared spectroscopy and compared to solution analogues to confirm the presence of [S]>SiH and [S]>$SiCo(CO)_4$ groups on the surface. The surface-confined [S]>$SiCo(CO)_4$ undergoes photoreactions that begin with loss of CO subsequent to optical excitation in the near-ultraviolet. The photochemistry closely parallels the behavior of solution $R_3SiCo(CO)_4$ analogoues; CO can be photosubstituted by $P(OPh)_3$ and the surface-confined [S]>$SiCo(CO)_3(P(OPh)_3)$ species is detectable by infrared spectroscopy. Irradiation of the oxide powders bearing [S]>$SiCo(CO)_4$ suspended in Et_3SiH solutions results in the release of the $-Co(CO)_4$ into solution as $Et_3SiCo(CO)_4$ concurrent with the regeneration of surface [S]>SiH functionality. Irradiation of the powders ([S]>$SiCo(CO)_4$) in the presence of 1-pentene yields $Co_4(CO)_{12}$ in solution and surface [S]>Si(pentenyl) groups. In the presence of Et_3SiH/1-pentene photoactivated catalysis by the derivatized powders ([S]>$SiCo(CO)_4$) occurs to give isomerization of the alkene, hydrosilation to give $Et_3Si(n\text{-pentyl})$, and small amounts of pentane. Reaction under H_2 improves the relative yield of pentane, while H_2/CO mixtures yield no hydroformylation products and lower the observed rate due to CO competing for the coordinatively unsaturated species. The surface [S]>SiH groups also add to 1-pentene to give powders bearing [S]>Si(*n*-pentyl) functionality. The use of powders functionalized with [S]>$SiCo(CO)_3(P(OPh)_3)$ also gives catalysis upon photoexcitation, but the product distribution differs significantly and includes at least two isomers of Et_3Si(pentenyl). In all cases the bulk of the catalysis appears to result from Co-carbonyl fragments photoreleased from the oxide support. The initial rate of catalysis appears to depend on the initial rate at which the fragments are released into homogeneous solution. The heterogeneous photocatalysts thus give the same product distribution as appropriate homogeneous precursors, but the oxide supported [S]>$SiCo(CO)_4$ is more easily isolated and handled and more durable than $R_3SiCo(CO)_4$.

Chemistry of surfaces modified with molecular reagents may have use in stoichiometric and catalytic syntheses, in adhesion and other surface physical tailoring, in analysis and separations, and in chemical energy conversion.[1-10] Successful application of molecular modification depends on characterization of both the structure and reactivity of the surface-confined species. One aim of research in this laboratory has been to initiate catalysis by optical excitation of thermally inert, surface-confined or-

† Dedicated to George S. Hammond on the occasion of his 60th birthday.

(1) Murray, R. W. *Acc. Chem. Res.* **1980**, *13*, 135.
(2) Karger, B. L.; Giese, R. W. *Anal. Chem.* **1978**, *50*, 1048A.
(3) (a) Arkles, B. *CHEMTECH* **1977**, 7, 766. (b) Whitehurst, D. D. *Ibid.* **1980**, *10*, 44.
(4) Bailey, D. C.; Langer, S. H. *Chem. Rev.* **1981**, *81*, 109.

0002-7863/81/1503-7180$01.25/0

ganometallic reagents. Thermally inert, surface-confined $-Fe(CO)_n$ reagents have been demonstrated to be photochemical precursors to catalysts for olefin isomerization and hydrosilation.[11] The anchoring surface for the $-Fe(CO)_n$ was a phosphinated polystyrene polymer, [P]– (refers to polymer support systems), where the organic polymer can be regarded as an insoluble, though solvent swellable, triarylphosphine ligand. For the [P]–$Fe(CO)_n$ system we found that the Fe–P anchor bond is sufficiently photoinert that olefin isomerization could be concluded to occur when the Fe–P bond is still intact. However, the polymer appeared to be sufficiently flexible that photogenerated coordinative unsaturation does not persist for extended periods. Further, it is likely that the [P]– system would be reactive to extensively coordinatively unsaturated Fe(O) species. Consequently, we have now turned attention to inorganic oxides as surfaces to which photochemical catalyst precursors can be attached. Inorganic oxides such as SiO_2 and Al_2O_3 should be inert, can be functionalized, and are transparent to ultraviolet and visible light over a wider range than for the [P]– system.

The system described in this article is the surface-confined [S]≻$SiCo(CO)_4$, where the [S]– is Al_2O_3 or SiO_2. The photochemistry and photocatalytic activity of $R_3SiCo(CO)_4$ (R = Et,Ph) have recently been described.[12] The [S]≻$SiCo(CO)_4$ materials are air stable at 25 °C for prolonged periods in contrast to $Et_3SiCo(CO)_4$, but the [S]≻$SiCo(CO)_4$ is very photosensitive. The photoactivity can be used to release catalytically active species into solution, but the primary photoprocess is CO release, not Co–Si bond cleavage. A preliminary communication has established that photochemical Si–Co bond cleavage does not occur; irradiation under ^{13}CO yields [S]≻$SiCo(CO)_n(^{13}CO)_{4-n}$, not the release of $Co(CO)_4$ to form $Co_2(CO)_n(^{13}CO)_{8-n}$.[13]

Studies of the surface of insulating metal oxides are not easily probed by surface-sensitive electron spectroscopies. We have made use of Fourier transform transmission infrared to characterize the surfaces functionalized with [S]≻SiH and [S]≻$SiCo(CO)_4$. This technique affords a molecular specific probe of structure and allows monitoring of the dilute catalytic sites of interest. As shown below, the surfaces of Al_2O_3 and SiO_2 that we have used for photocatalysis have many surface functionalities present. As in solution, we exploit the fact that a chromophore, [S]≻$SiCo(CO)_4$, present in dilute amounts can be selectively activated by light. This represents one of the major advantages for optical vs. thermal activation of catalysis; in principle, the activation energy can be deposited selectively into the sites that are active.

Experimental Section

Physical Measurements and Analysis. Infrared spectra of surfaces were taken as KBr pellets (~10% Al_2O_3 or SiO_2) on a Perkin-Elmer Model 180 dispersion or a Nicolet 7199 Fourier transform spectrometer. Solutions were analyzed in matched 1.0-mm or 0.1-mm path length sealed NaCl cells. Electronic spectra of solutions were obtained on a Cary 17 UV–vis–near-IR spectrophotometer in 1.00-cm quartz or 1.00-cm Pyrex cells. Gas chromatographic analyses were performed on a Varian Model 1440 or 2440 gas chromatograph equipped with flame ionization detectors and interfaced with a Hewlett-Packard Model 3370S recording integrator. Hydrocarbon products were analyzed at 20 °C on columns of 20% propylene carbonate on Chromosorb P (Johns-Manville, $^1/_8$ in. × 30 ft) against an internal standard, hexane. Hydrosilation products were analyzed at 60 °C on columns of 20% β,β′-oxydipropionitrile (Applied Science Laboratories, $^1/_8$ in. × 30 ft) against an internal standard, decane. Authentic samples of all products were available for calibration of the detector response and for retention time comparisons.

Reaction Conditions. All manipulations of O_2- and H_2O-sensitive materials were performed in a Vacuum Atmospheres He-43-6 Dri-Lab glovebox with an attached HE-493 Dri-Train or in conventional Schlenk glassware under an N_2 atmosphere. Samples for irradiation were freeze–pump–thaw degassed at least four times in 13-mm o.d. Pyrex ampules containing 2 mm × 7 mm Teflon-coated magnetic stirring bars and sealed hermetically under vacuum (10^{-5} torr). Reactions under H_2 were performed in 13-mm o.d. Pyrex tubes fused to ground-glass joints, which were connected to a source of vacuum and of H_2. The system was flushed at least four times with H_2 before H_2 gas was admitted to the sample under vacuum. Irradiations were performed with a medium-pressure Hg arc lamp (Hanovia, 450 W) fitted with a supplementary H_2O filter to remove infrared radiation or at lower intensities with two General Electric #F15T8/BLB Black Lites (λ_{max} = 355 ± 20 nm; ~2 × 10^{-6} einstein/min as determined by ferrioxalate actinometry).[14]

Materials. Chromatographic grade $SiO_x{\cdot}xH_2O$ (Davison Chemical Co., 80–200 mesh) was used as received. Chromatographic grade neutral Al_2O_3 (Woelm grade I) was activated for 24 h at 450 °C before use and stored in the drybox. High surface area γ-Al_2O_3 (200 m^2/g, Strem) was received as pellets and used as received or pulverized before use in some experiments. Powdered, high surface area SiO_2 (400 m^2/g, Alfa) was used as received. 1-pentene (99%, Phillips Chemical Co.) and $HSiEt_3$ (Petrarch) were passed through activated Al_2O_3 prior to use and stored in amber bottles at 4 °C. Triphenylsilane (Petrarch) was recrystallized from pentane prior to use. Triethoxysilane (Petrarch) was freeze–pump–thaw degassed upon receipt and stored in the drybox. $Co_2(CO)_8$ (Strem), hexane (Aldrich), decane (Aldrich), $HSiCl_3$ (Aldrich), and Me_2ClSiH (Petrarch) were used as received. $R_3SiCo(CO)_4$ (R = Et, Ph) were prepared as previously described and stored at 0 °C under N_2.[12] $Co_4(CO)_{12}$ was prepared by heating $Co_2(CO)_8$ in isooctane at 80–90 °C for 12 h. The product was filtered off, recrystallized from benzene/isooctane, and stored at 0 °C under N_2. Hydrocarbon solvents were distilled from CaH_2 under N_2; THF was distilled from Na/benzophenone under N_2.

Derivatization of Oxide Supports. A typical procedure is outlined. A 1.6-mL sample $HSi(OEt)_3$ in 10 mL of isooctane under N_2 was added to 4 g of powdered Al_2O_3 in a Schlenk tube. In some cases, 0.12 mL of distilled H_2O was added via syringe. The suspension was allowed to stand at 25 °C under slow N_2 purge for 12–36 h with periodic agitation, after which time excess solution was drained off. In some cases, the [S]≻SiH derivatized surface was washed with hexanes and isolated at this stage. Under N_2, a solution of 1.4 g of $Co_2(CO)_8$ in 10 mL of isooctane was added by syringe. After 12 h at 25 °C under slow N_2 purge with intermittent agitation, the tube was opened in the dark. The derivatized powder was washed with a copious quantity of hexanes or pentane until the rinsings were colorless. The derivatized powder was dried under vacuum at 25 °C.

Functionalization using Me_2ClSiH was carried out in a manner similar to that for Cl_3SiH or $(EtO)_3SiH$ except that dry Et_3N was added. A typical procedure was to react 2 g of Al_2O_3 or SiO_2 with 5 mL of Me_2ClSiH and 4 mL of Et_3N in 50 mL of isooctane for 24 h at 20 °C. The excess Me_2ClSiH, Et_3N, and isooctane were stripped off under vacuum. The solid was washed with isooctane leaving the [S]–$SiMe_2H$ and the $Et_3N{\cdot}HCl$. The $Et_3N{\cdot}HCl$ was removed by washing with CH_2Cl_2 and again with isooctane. To further functionalize to form [S]–$SiMe_2Co(CO)_4$ the [S]–$SiMe_2H$ was reacted with excess $Co_2(CO)_8$ in isooctane under N_2 for 22 h at 20 °C. The solid was washed with isooctane and dried under vacuum.

The surface [S]≻SiH and [S]≻$SiCo(CO)_4$ are infrared detectable (Table I). Typical analyses were performed by making measurements of KBr pellets containing [S]≻SiH and/or [S]≻$SiCo(CO)_4$ (~10% by weight). The pellets are made in as reproducible a fashion as possible. A 200-mg sample of dry, infrared grade KBr and 20 mg of [S]≻SiH or [S]≻$SiCo(CO)_4$ are first ground together with a mortar and pestle until a homogeneous powder results. The pellet is then pressed in a KBr die at 20 000 psi for 5 min to yield a pellet of 1.00-cm diameter and 0.05-cm thickness. Absorptivity of model compounds Ph_3SiH (ν_{Si-H} = 2118 cm^{-1} in KBr) and $Ph_3SiCo(CO)_4$ (ν_{C-O} = 2092, 2030, 1990 cm^{-1} in KBr) was determined in KBr and reproducibility was determined to be ±20%. Errors for samples including the SiO_2 or Al_2O_3 are even larger. The semiquantitative infrared measurements show [S]≻$SiCo(CO)_4$ to be air-stable at 25 °C for at least several weeks. The relative absorptivities in Table I, relative to Ph_3Si-H (ν_{Si-H} = 2118 cm^{-1}) are proportional to concentration and can thus be used to determine concentrations of the [S]≻SiH or [S]≻$SiCo(CO)_4$. The relative absorbance of 1.0 for the 2118-cm^{-1} Si–H stretch in Ph_3SiH corresponds to an absolute absorptivity of 1.0–o.d. unit for a 2.54:100 weight ratio of Ph_3SiH to KBr in

(5) Hartley, F. R.; Vezey, P. N. *Adv. Organomet. Chem.* **1977**, *17*, 189.
(6) Grushka, E.; Kikta, E. J. *Anal. Chem.* **1977**, *49*, 1004A.
(7) Collman, J. P.; Denisevich, P.; Konai, Y.; Marrocco, M.; Koval, C.; Anson, F. C. *J. Am. Chem. Soc.* **1980**, *102*, 6027.
(8) Degrand, C.; Miller, L. L. *J. Am. Chem. Soc.* **1980**, *102*, 5728.
(9) Bolts, J. M.; Bocarsly, A. B.; Palazzotto, M. C.; Walton, E. G.; Lewis, N. S.; Wrighton, M. S. *J. Am. Chem. Soc.* **1979**, *101*, 1378.
(10) Bookbinder, D. C.; Bruce, J. A.; Dominey, R. N.; Lewis, N. S.; Wrightin, M. S. *Proc. Natl. Acad. Sci. U.S.A.* **1980**, *77*, 6280.
(11) Sanner, R. D.; Austin, R. G.; Wrighton, M. S.; Honnick, W. D.; Pittman, C. U., Jr. *Inorg. Chem.* **1979**, *18*, 928.
(12) Reichel, C. L.; Wrighton, M. S. *Inorg. Chem.* **1980**, *19*, 3858.
(13) Kinney, J. B.; Staley, R. H.; Reichel, C. L.; Wrighton, M. S. *J. Am. Chem. Soc.* **1981**, *103*, 4273.
(14) Hatchard, C. G.; Parker, C. A. *Proc. R. Soc. London, Ser. A* **1956**, *235*, 518.

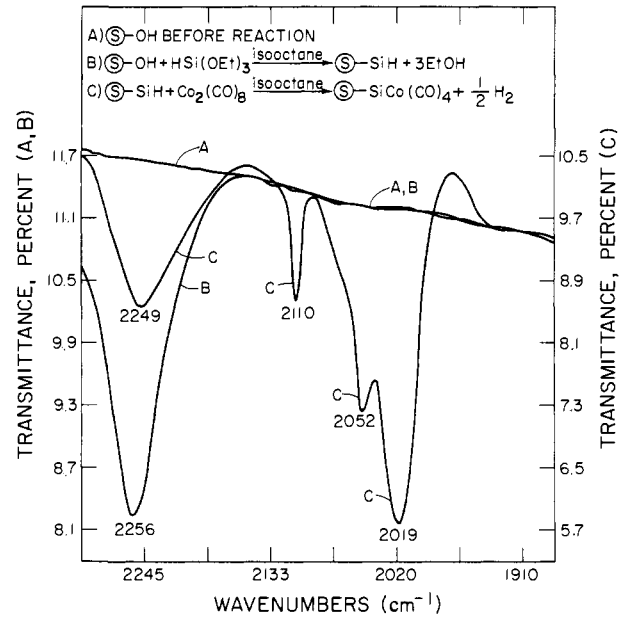

Figure 1. Infrared spectral changes accompanying the progressive derivatization of a naked alumina surface. curve A refers to the surface before reaction, curve B to the surface after reaction with $HSi(OEt)_3$, and curve C to the surface after reaction with $HSi(OEt)_3$ and subsequently $Co_2(CO)_8$. Note that left scale is for A and B and right scale is for C.

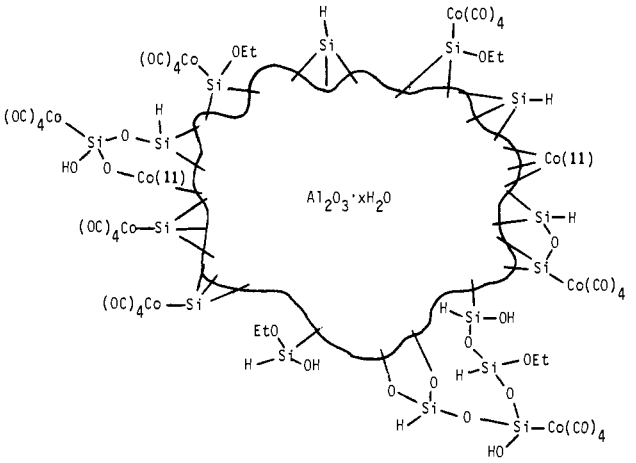

Figure 2. Representation of derivatized $Al_2O_3 \cdot xH_2O$ prepared in this work.

our 1.0-cm diameter, 0.05 cm thick, pellets prepared as described above. Thus, the relative absorbance of 5.5 for ν_{C-O} = 2092 cm^{-1} of $Ph_3SiCo(CO)_4$ means that the absorptivity is 5.5 times that of the 2118-cm^{-1} Si–H stretch of Ph_3SiH for the same number of moles in a given mass of KBr.

To ensure that KBr is not reactive when used as a pellet material, we have recorded the infrared spectrum of [S]>$SiCo(CO)_4$ and [S]>SiH in Nujol mulls. The relative absorptivities are the same as in KBr pellets. Also, the infrared absorbances in KBr are proportional to the signals from Fourier transform infrared photoacoustic spectroscopy of the [S]->$SiCo(CO)_4$ powders.[13]

Results and Discussion

a. Surface Derivatization and Characterization. The synthesis of [S]>$SiCo(CO)_4$ depends on two previous synthetic procedures, eq 1[3] and 2.[15]

$$(EtO)_3SiH + \text{surface—OH} \longrightarrow \text{surface—O—SiH} + 3EtOH \quad (1)$$

$$2R_3SiH + Co_2(CO)_8 \rightarrow 2R_3SiCo(CO)_4 + H_2 \quad (2)$$

The Al_2O_3 and SiO_2 generally have variable amounts of surface–OH depending on prior history of the samples. We have synthesized [S]>$SiCo(CO)_4$ by exploiting the chemistry represented by eq 1 and 2 and have characterized the surfaces by transmission infrared spectroscopy. Representative infrared spectra [S]>$SiCo(CO)_4$, [S] = Al_2O_3, synthesis are shown in Figure 1. The Al_2O_3 is featureless in the Si–H and C–O stretching region. Treatment with $(EtO)_3SiH$ results in a priminent spectral feature at ~2250 cm^{-1}. We associate this feature with the Si–H stretch for the surface-confined groups. Reaction of the [S]>SiH powder with $Co_2(CO)_8$ results in a powder that has infrared absorption at ~2110, ~2050, and ~2020 cm^{-1} in accord with a [S]>$SiCo(CO)_4$ system. Note that while we generally find some diminution in the absorption associated with the Si–H stretch, it is not completely absent even after exhaustive reaction with $Co_2(CO)_8$. Table I lists infrared absorptions for [S]>SiH, [S]>$SiCo(CO)_4$, and various other systems of relevance to results described below. Included in Table I are data from experiments using Cl_3SiH or Me_2ClSiH, rather than $(EtO)_3SiH$, to introduce >SiH functionality on the surface.

Infrared spectroscopy (Table I) reveals the presence, but not the uniformity of coverage, of >SiH and >$SiCo(CO)_4$ on Al_2O_3 and SiO_2. The characteristic absorption associated with the >SiH is in the range 2134–2257 cm^{-1}, depending on the oxide (Al_2O_3 or SiO_2), the starting silane ($(EtO)_3SiH$, Cl_3SiH, or Me_2ClSiH), and the derivatization conditions (H_2O added or not added). A large range of Si–H stretching frequencies is also found for the various silanes measured in alkane solution. Generally, the Si–H stretching frequency would be expected to be a function of the three remaining groups bonded to the Si atom. The largest difference for surface Si–H stretching frequencies comes from the use of Me_2ClSiH, $\nu_{Si-H} \approx 2140$ cm^{-1}, compared to using either Cl_3SiH or $(EtO)_3SiH$, $\nu_{Si-H} \approx 2250$ cm^{-1}. The ~100-sm^{-1} difference is attributable to the presence of the two alkyl groups on the surface Si when using Me_2ClSiH whereas the Cl_3SiH or $(EtO)_3SiH$ likely results in only oxygen linkages to the surface Si. The value of ν_{Si-H} for polymeric material from the reaction of H_2O with $(EtO)_3SiH$ or Cl_3SiH accords well with the surfaces derivatized with these reagents. Essentially complete hydrolysis of the $(EtO)_3SiH$ is inferred from the very small signals for C–H stretching absorptions (from EtO–groups) for Al_2O_3 or SiO_2 functionalized with $(EtO)_3SiH$. For Me_2ClSiH the retention of the methyl groups is directly confirmed by the observation of a C–H stretching absorption at 2985 cm^{-1} for the derivatized surfaces; Me_2ClSiH shows a C–H stretch at 2965 cm^{-1} in CCl_4 solution. The value of ν_{Si-H} for Me_2ClSiH, Cl_3SiH, $(EtO)_3SiH$, and the other Si–H containing materials is consistent with the retention of the two methyl groups when using Me_2ClSiH to functionalize the surface.

Spectral features attributable to the $-Co(CO)_4$ are also dependent on the nature of the group bonded to the Co. The variation in the CO stretching frequencies for $(EtO)_3SiCo(CO)_4$, $Et_3SiCo(CO)_4$, and $Ph_3SiCo(CO)_4$ accord well with the variation for [S]>$SiCo(CO)_4$ depending on whether Me_2ClSiH vs. Cl_3SiH or $(EtO)_3SiH$ is used as the Si–H source. The two alkyl groups on the Si release electron density (compared to three oxygen groups) such that the ν_{C-O} is moved to lower energy presumably reflecting greater π-back-bonding to CO from the more electron-rich Co. Thus, for both >SiH and $-Co(CO)_4$ some molecular level information can be deduced from the infrared spectroscopy. But small differences in band position should not be overinterpreted, since the bands are relatively (compared to solutions) broad. Even for the same sample, some variation (±3 cm^{-1}) in band maxima can be found from KBr pellet to KBr pellet.

By measuring the absorbance associated with [S]>SiH ($\nu_{Si-H} \approx 2250$ cm^{-1}) and [S]>$SiCo(CO)_4$ ($\nu_{CO} \approx 2025$ cm^{-1}) for KBr pellets, we have estimated the amount of >SiH and >$SiCo(CO)_4$ confined to the oxide surfaces. Results from various preparation

(15) Chalk, A. J.; Harrod, J. F. *J. Am. Chem. Soc.* **1967**, *89*, 1640.

Table I. Infrared Spectra of Surface-Confined Species and Relevant Species for Comparison

species	medium	key IR band(s), cm^{-1} (ϵ or rel abs)[d]
$(EtO)_3SiCo(CO)_4$[a]	heptane	2105 (0.29), 2040 (0.81), 2025 (0.86), 2010 (1.00)
$Et_3SiCo(CO)_4$	cyclohexane	2089 (2740), 2026 (4390), 1995 (8580), 1992 sh (8000)
$Ph_3SiCo(CO)_4$	cyclohexane	2093 (3250), 2032 (3720), 2003 (7000)
	KBr[b]	2092 (*5.5*),[b] 2030 (*5.5*),[b] 1990 (*7.4, 7.7*)[b]
$Ph_3SiCo(CO)_3(P(OPh)_3)$[c]	cyclohexane	2049 (0.11), 1980 (0.82), 1973 (1.00)
$Et_3SiCo(CO)_3(P(OPh_3)$[c]	hexane	2035 (0.35), 1968 (0.98), 1963 (1.00)
$(EtO)_3SiCo(CO)_3(P(OPh)_3)$[c]	isooctane	1987 (1.00), 1974 (0.78)
$Co_4(CO)_{12}$	cyclohexane	2062 (12 550), 2053 (14 000), 2037 (930), 2025 (1590), 2020 sh (930), 1864 (4890)
Ph_3Si-H	cyclohexane	2129 (204)
	isooctane	2126 (214)
	KBr[b]	2118 (*1.0*)[b]
$(EtO)_3Si-H$	isooctane	2196 (135)
	neat	2195 (...)
Et_3Si-H	isooctane	2100 (149)
Cl_3Si-H	heptane	2250 (...)
$Me_2ClSi-H$	isooctane	2165 (223)
$[O_3Si-H]_n$ (from $(EtO)_3SiH + H_2O$)	neat	2246
	Nujol mull	2253
	KBr	2256
$[O_3Si-H]_n$ (from $Cl_3SiH + H_2O$)	Nujol mull	2252
[S] ⩾ SiH (from$(EtO)_3SiH$)	KBr	
[S] = Al_2O_3		2257 (H_2O added); 2239 (dry)
[S] = SiO_2		2248 (dry)
[S] ⩾ $SiCo(CO)_4$ (from $(EtO)_3SiH$)	KBr	
[S] = Al_2O_3 (dry)		2109 (0.27), 2051 (0.58), 2023 (1.00)
[S] = Al_2O_3 (H_2O added)		2111 (0.40), 2054 (0.66), 2024 (1.00)
[S] = SiO_2		2108 (0.29), 2048 (0.51), 2020 (1.00)
[S] ⩾ $SiCo(CO)_3(P(OPh)_3)$	KBr	
[S] = Al_2O_3		2060 (0.21), 1995 (1.00), 1985 (0.91)
[S] = SiO_2		2059 (0.10), 1991 (1.00), 1983 (0.99)
[S] ⩾ SiH (from $HSiCl_3$)	KBr	
[S] = Al_2O_3		2263 (H_2O added); 2257 (dry)
[S] ⩾ $SiCo(CO)_4$ (from $HSiCl_3$)	KBr	
[S] = Al_2O_3		2114 (0.30), 2054 (0.49), 2025 (1.00)
[S] ⩾ $SiMe_2H$ (from Me_2ClSiH)	KBr	
[S] = Al_2O_3		2134
[S] = SiO_2		2148
[S] ⩾ $SiMe_2Co(CO)_4$ (from Me_2ClSiH)	KBr	
[S] = SiO_2		2100 (0.25), 2039 (0.48), 2009 (1.00)

[a] Generated *in situ* by reaction of $Co_2(CO)_8$ with $(EtO)_3SiH$ in heptane. [b] Italic values in parentheses are for "model" complexes in KBr relative to the 2118-cm^{-1} Si-H stretch in Ph_3SiH. O.d. was determined to be proportional to concentration in KBr; cf. Experimental Section. These Absorptivities are absolute and allow the coverage calculations for ⩾$SiCo(CO)_4$ and ⩾SiH by assuming similar absorptivities for the various bands (Table II). [c] Generated in situ by 355-nm irradiation of appropriate $R_3SiCo(CO)_4$ in the presence of 0.01 M $P(OPh)_3$; cf. ref 12. [d] Values in parentheses are relative absorbance (relative to most intense band for the substance equal to 1.00), extinction coefficient in solutions, or quantitative absorbance relative to Ph_3SiH; cf. Experimental Section and footnote *b* above.

procedures using various sources of Al_2O_3 give qualitatively similar results (Table II). Note that ⩾SiH persists in every case; some of this functionality may be either structurally or mechanistically inaccessible to the $Co_2(CO)_8$. The data for the high surface area (200 m^2/g) γ-Al_2O_3 pellets, sample no. 1 in Table II, allow a calculation of *average* coverage of ⩾SiH and ⩾$SiCo(CO)_4$ assuming all of the surface area to be accessible. We calculate an average coverage of $\sim 10^{-12}$ mol of ⩾$SiCo(CO)_4$ and $\sim 3 \times 10^{-11}$ mol of ⩾SiH/cm^2 of surface. Similar coverages are found for the high surface area (400 m^2/g) SiO_2, sample no. 8 of Table II. Taking $\sim 10^{-10}$ mol/cm^2 to be a monolayer, we find monolayer to submonolayer coverage to be a typical result. The coverages from infrared spectroscopy are very approximate, perhaps correct within a factor of 3. There are many sources of error including the fact that absorptivities for the Si–H stretch vary considerably (Table I), depending on the environment around the Si and the medium in which the ⩾SiH is dispersed or dissolved. But the qualitative finding of monolayer or submonolayer coverage is in accord with determinations of coverage of other functionality, albeit larger groups, using hydrolytically unstable silane reagents.[16] It is noteworthy that –OH absorption in the infrared does not disappear upon functionalization of the oxide powders with either $(EtO)_3SiH$ or the more reactive Cl_3SiH. Some of the –OH after derivatization could be due to $-Si(H)(OH)_x$ from the hydrolysis of the $(EtO)_3SiH$ or Cl_3SiH. Further, it is unlikely that all –OH associated with the hydrated oxides is accessible.

While it may be attractive to conclude that $(EtO)_3SiH$ or Cl_3SiH functionalize the oxide with a uniform monolayer or less of ⩾SiH, such is unlikely. The $(EtO)_3SiH$ and Cl_3SiH can polymerize and such is known to occur when using $(RO)_3SiR'$ or Cl_3SiR' reagents for modifying chromatographic supports or electrode materials.[1,2,9] Indeed, unless H_2O can be completely removed the polymerization is probably unavoidable. Removing all of the H_2O would also mean dehydrating the oxides, and coverage of the ⩾SiH on the anhydrous oxides would likely be low. Functionalization of the Al_2O_3 or SiO_2 with Me_2ClSiH provides some indirect information concerning the polymerization, since Me_2ClSiH is not capable of forming the polymers. Surfaces derivatized with Me_2ClSiH have an amount of ⩾SiH, based on infrared absorption, that is not qualitatively different than that from derivatization with Cl_3SiH or $(EtO)_3SiH$. This likely means polymerization from Cl_3SiH or $(EtO)_3SiH$ is not extensive. At least, we find that the results are consistent with rather uniform, low coverage of ⩾SiH independent of the source of ⩾SiH. However, as indicated above, the Me_2Si-H is electronically different from the ⩾SiH where the three groups bonded to the Si are oxygen.

Another complication in the attachment of $-Co(CO)_4$ to the oxide supports is that $Co_2(CO)_8$ reacts rapidly with Lewis bases

(16) Fischer, A. B.; Kinney, J. B.; Staley, R. H.; Wrighton, M. S. *J. Am. Chem. Soc.* **1979**, *101*, 6501.

Table II. Typical Coverages of ≥SiH and ≥$SiCo(CO)_4$ Synthesized by Various Procedures[a]

oxide	sample no.	procedure[b]	analysis from infrared[c] mol % of SiH	analysis from infrared[c] mol % of $SiCo(CO)_4$	elemental analyses[d] % Si (calcd)	elemental analyses[d] % Co (calcd)
γ-Al_2O_3 (powdered)[e]	0	not derivatized	0	0	0.09 (0)	<0.009 (0)
	0''	III, but no $Co_2(CO)_8$	4.00	0	3.03 (1.15)	0 (0)
	0'''	III, but no $Co_2(CO)_8$	2.86	0	3.43 (0.81)	0 (0)
γ-Al_2O_3 (pellets)	1	I	1.3	0.05	2.16 (0.36)	0.84 (0.03)
	1'	I, but no $Co_2(CO)_8$	1.99	0	2.62 (0.56)	0 (0)
	1''	I	1.6	0.14	2.53 (0.49)	0.47 (0.08)
γ-Al_2O_3 (powdered)[e]	2	II	2.7	0.4	2.51 (0.90)	0.72 (0.25)
	3	III	2.7	0.9		
	4	IV	1.1	0.2		
	5	V	1.3	0.4	3.66 (0.50)	1.03 (0.25)
	6	VI	2.4	0.5		
Woelm Al_2O_3	7	not derivatized	0	0	0.05 (0)	<0.009 (0)
	7'	III	0.5	0.03	2.06 (0.15)	0.55 (0.02)
SiO_2 (400 m^2/g)	8	VII	2.92 (prior to $Co_2(CO)_8$)	...		
			2.88 (after $Co_2(CO)_8$)	0.25		
	8'	IV	6.1 (prior to $Co_2(CO)_8$)	...		
			3.4 (after $Co_2(CO)_8$)	1.9		
Al_2O_3 (powdered)[e]	9	VII	0.15 (prior to $Co_2(CO)_8$)	...		
			0.15 (after $Co_2(CO)_8$)	detectable		

[a] Derivatization procedure is generally Al_2O_3 [$(EtO)_3SiH$, 25 °C] → [$Co_2(CO)_8$, 25 °C] →. [b] I, derivatized under anhydrous conditions; the [S]≥SiH intermediate was not isolated prior to $Co_2(CO)_8$ reaction. II, same as I but a very large excess (25× vs. usual 5×) of $(EtO)_3SiH$ was used. III, same as II but H_2O (0.12 mL) added during reaction with $(EtO)_3SiH$. IV, same as I but [S]≥SiH was isolated prior to reaction. V, same as IV but H_2O (0.12 mL) added during reaction with $(EtO)_3SiH$. VI, same as V but very large excess of $(EtO)_3SiH$ was used. VII, functionalized with Me_2ClSiH as in Experimental Section. [c] Coverages are approximated by infrared spectroscopy, 2250 cm^{-1} for ≥Si-H and ~2020 cm^{-1} for ≥$SiCo(CO)_4$, see Table I and Experimental Section. The mol % refers to the ratio moles of SiH or $SiCo(CO)_4$ to moles of SiO_2 or Al_2O_3 times 100%. [d] Elemental analyses (Galbraith) for Si and Co (% by weight) were performed for some of the samples. The % by weight of Si and Co from the infrared data are given in parentheses. These calculated values would be for Co as ≥$SiCo(CO)_4$ and Si as ≥SiH plus ≥$SiCo(CO)_4$. The Co and Si present as oxide from decomposition is thus significant, see text. [e] Powdered γ-Al_2O_3 is from pulverized γ-Al_2O_3 pellets of 200 m^2/g surface area.

to give redox products.[17] For example, we find that Al_2O_3 reacts with $Co_2(CO)_8$ to give a bluish powder. This bluish color also appears when the Al_2O_3 has been first treated with $(EtO)_3SiH$ to introduce ≥SiH surface groups prior to reaction with $Co_2(CO)_8$. We attribute the bluish color to Co^{2+} on the surface; this was confirmed by reacting the $Co_2(CO)_8$ treated Al_2O_3 with aqueous 1 M HCl. The resulting pink solution showed optical absorption spectral features identical with those for an autneitic Co^{2+} sample in aqueous 1 M HCl: λ_{max} 1250, 510, 463 sh nm.[18] The $Co_2(CO)_8$-treated Al_2O_3 shows no C–O infrared stretches attributable to surface-confined metal carbonyls. We thus conclude that $Co_2(CO)_8$ reacts with Al_2O_3 to yield a cobalt oxide/hydroxide. Thus, cobalt oxide formation appears as a side reaction accompanying the attachment of $-Co(CO)_4$ by reaction of $Co_2(CO)_8$ with the [S]≥SiH groups.

Elemental analyses for some of the Al_2O_3 samples are included in Table II. Nonderivatized samples show little or no detectable Co or Si, and samples derivatized with $(EtO)_3SiH$ but not with $Co_2(CO)_8$ show the presence of Si but not Co, as expected. The comparison of the elemental analyses with the infrared analyses is revealing. There is apparently far more Si present than can be accounted for by the ≥SiH and ≥$SiCo(CO)_4$. Further, there is far more Co present that can be accounted for by ≥$SiCo(CO)_4$. The infrared determined coverages of ≥$SiCo(CO)_4$ are consistent (±20%) with the amounts of $Et_3SiCo(CO)_4$ that can be detected in solution when [S]≥$SiCo(CO)_4$ is irradiated in isooctane as a suspension in the presence of Et_3SiH (*vide infra*). Thus, the excess Co from the analyses must be due to the cobalt oxide/hydroxide formed from the decomposition of $Co_2(CO)_8$ in the derivatization procedure. Though we do not have a check of ≥SiH as we do for ≥$SiCo(CO)_4$, it would seem that the error in % Si from infrared detectable ≥SiH cannot be as large as would be necessary to account for the % Si from elemental analyses. We propose that decomposition of ≥SiH occurs, perhaps by acid–base reactions, to give silicate on the surface. Reaction with $Co_2(CO)_8$ could lead to decomposition of ≥SiH, but even surfaces that have not been treated with $Co_2(CO)_8$ give more Si than can be detected as ≥SiH by infrared. A major conclusion from these results is that neither elemental analyses nor infrared alone can provide quantitative information concerning the surface functionality present.

From our studies, we conclude that the derivatized oxide particles have a large number of chemical functionalities present. The representation of a derivatized alumina particle in Figure 2 seems justifiable in view of the available infrared data and known reactions. Despite the large number of chemical functionalities, light-activated reactions of the ≥$SiCo(CO)_4$ can still be studied, owing to the facts that this group can absorb incident light and reactions of this metal carbonyl fragment can be monitored in the C–O stretching region of the infrared without interference from other groups. Photoexcitation of [S]≥$Co(CO)_4$, though it is present in dilute amounts, is analogous to optical excitation of substances in solution at low concentration, exploiting one of the key advantages in optical vs. thermal activation of chemical systems. The absorption onset of [S]≥$SiCo(CO)_4$ is expected to occur in the near-UV, on the basis of solution analogues, and consequently, photochemical studies have been carried out by using near-UV ($\lambda > 300$ nm) light.

b. Photochemistry of [S]≥$SiCo(CO)_4$ in the Presence of P(OPh)$_3$. Irradiation of deoxygenated 3.0-mL isooctane suspensions of 0.045 g of [S]≥$SiCo(CO)_4$, sample no. 3 in Table II, in the presence of 0.01 M $P(OPh)_3$ yields reactions according to eq 3.

$$[S]{\geq}SiCo(CO)_4 \xrightarrow[\text{isooctane}]{\text{near-UV, 0.01 M } P(OPh)_3} [S]{\geq}SiCo(CO)_3(P(OPh)_3) + CO \quad (3)$$

Infrared analysis of the supernatant liquid shows no metal carbonyl species. The formation of $Co_2(CO)_6(P(OPh)_3)_2$ would be possible if light-induced cleavage of the Si–Co bond resulted followed by substitution of the released $Co(CO)_4$ radical by $P(OPh)_3$ to yield $Co(CO)_3(P(OPh)_3)$ radicals that then couple to form $Co_2(CO)_6(P(OPh)_3)_2$.[19] Infrared analysis of the powder after various

(17) Wender, I.; Sternberg, H. W.; Orchin, M. *J. Am. Chem. Soc.* **1952**, *74*, 1216.
(18) Figgis, B. N. "Introduction to Ligand Fields"; Wiley: New York, 1966; p 223.
(19) Brown, T. L.; Absi-Halabi, M. *J. Am. Chem. Soc.* **1977**, *99*, 2982.

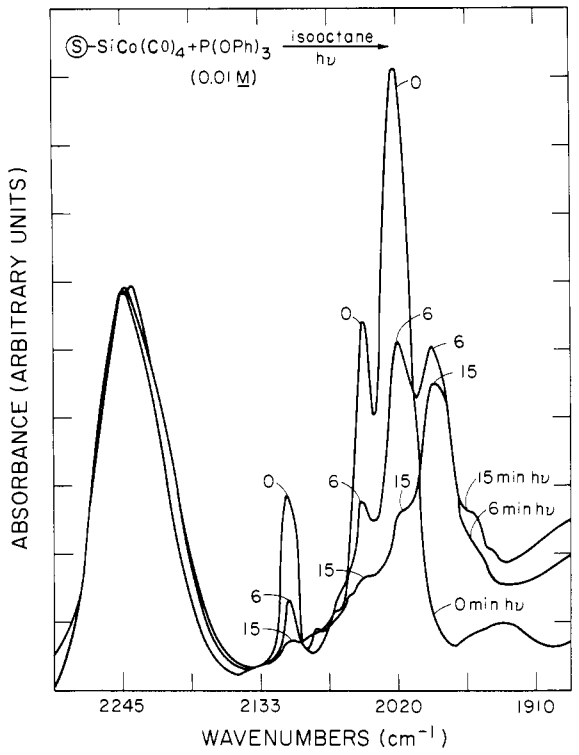

Figure 3. Infrared spectral changes during the irradiation of a derivatized alumina surface in the presence of $P(OPh)_3$. The only CO-containing product is $\geq SiCo(CO)_3(P(OPh)_3)$ (1995 (vs), 1985 (vs) cm^{-1}).

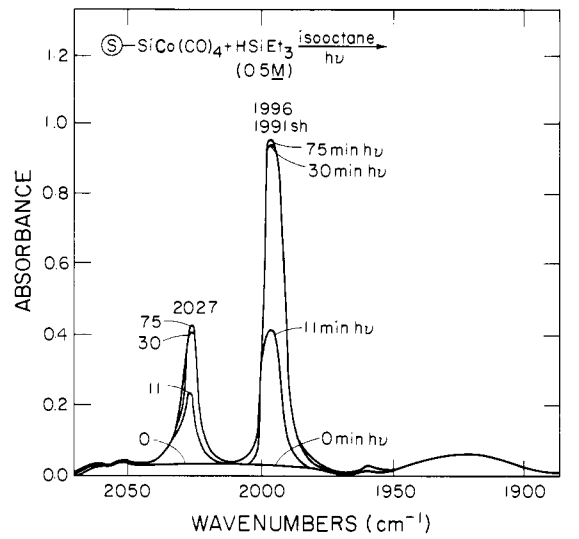

Figure 4. Infrared spectral changes in solution during the irradiation of $[S]\geq SiCo(CO)_4$, [S] = Al_2O_3 in the presence of $HSiEt_3$. The only detectable photoproduct in solution is $Et_3SiCo(CO)_4$ (2027, 1996, 1991 (sh) cm^{-1}).

irradiation times (Figure 3) shows the diminution of absorptions attributable to the $[S]\geq SiCo(CO)_4$ and the growth of features that are assigned to $[So]\geq SiCo(CO)_3(P(OPh)_3)$ (Table I). Thus, it appears that CO can be photochemically ejected from $[S]-\geq SiCo(CO)_4$ and Si–Co bond cleavage is apparently unimportant.

Irradiation of $[S]\geq SiCo(CO)_4$ in isooctane solution containing no deliberately added entering groups results in the diminution of metal carbonyl absorption in the C–O stretching region. An unidentifiable absorption feature does grow in at 2073 cm^{-1} as a shoulder at intermediate stages of reaction, but the surface would appear to be eventually denuded of metal carbonyls by the near-UV irradiation. The isooctane supernatant exhibits infrared absorptions at positions characteristics of $Co_4(CO)_{12}$ (Table I). The yield of this species appears to be ~15%. Both these data and data for photochemistry in the presence of $P(OPh)_3$ parallel

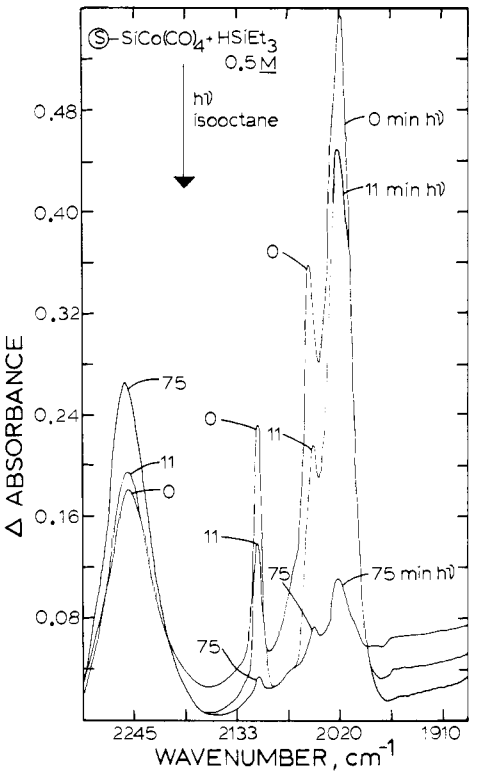

Figure 5. Infrared spectral changes of a derivatized Al_2O_3 surface accompanying irradiation in the presence of $HSiEt_3$. $\geq SiCo(CO)_4$ (2110, 2050, 2020 cm^{-1}) is removed from the surface while the $\geq SiH$ concentration (2250 cm^{-1}) increases.

the photochemical data for $R_3SiCo(CO)_4$ in solution.[12]

c. Photochemistry of $[S]\geq SiCo(CO)_4$ in the Presence of Et_3SiH. Underconditions where CO is photolabilized, irradiation of suspended $[S]\geq SiCo(CO)_4$ in the presence of Et_3SiH results in the detachment of the $-Co(CO)_4$ from the surface. For example, degassed, 3.0-mL isooctane solutions containing 0.045 g of $[S]-\geq SiCo(CO)_4$, sample no. 3 of Table II, and 0.5 M Et_3SiH under near-UV irradiation at 25 °C yield $Et_3SiCo(CO)_4$ in the supernatant isooctane solution (Figure 4). Analysis of the irradiated powder reveals the decline of absorptions due to metal carbonyl fragments (Figure 5). The only feature that grows is one at ~2250 cm^{-1} attributable to the regeneration of $[S]\geq SiH$. Infrared analysis shows that >80% of the surface-confined $-Co(CO)_4$ fragments can be detected as $Et_3SiCo(CO)_4$ in solution. Such data provide confirmation of the coverages of surface-confined $Co(CO)_4$ groups given in Table II. The photochemistry again can be rationalized as resulting from photoinduced loss of CO as the primary photoprocess according to eq 4–7, paralleling the solution photochemical behavior of $R_3SiCo(CO)_4$.[12]

$$[S]\geq SiCo(CO)_4 \overset{h\nu}{\rightleftharpoons} [S]\geq SiCo(CO)_3 + CO \quad (4)$$

$$[S]\geq SiCo(CO)_3 + Et_3SiH \rightleftharpoons [S]\geq Si(H)-Co(CO)_3(SiEt_3) \quad (5)$$

$$[S]\geq Si(H)Co(CO)_3(SiEt_3) \rightleftharpoons [S]\geq SiH + Et_3SiCo(CO)_3 \quad (6)$$

$$Et_3SiCo(CO)_3 + CO \rightarrow Et_3SiCo(CO)_4 \quad (7)$$

d. Photochemistry of $[S]\geq SiCo(CO)_4$ Related to Alkene Catalysis. We have previously reported that $R_3SiCo(CO)_4$ is a photochemical precursor to catalytically active species,[12] despite the fact that Si–Co bond cleavage is not the primary photoprocess. Near-UV irradaition of $[S]\geq SiCo(CO)_4$ in isooctane solutions

Table III. Photocatalyzed Reactions of 1-Pentene[a]

	initial conditions				product distribution, % of total				
hν, min	1-pentene, M	$HSiEt_3$, M	H_2, psig	CO, psig	*n*-pentane	1-pentene	*trans*-2-pentene	*cis*-2-pentene	Et_3Si(*n*-pentyl)
120	3.26	3.26	4	0	10.2	2.4	60.7	17.1	9.7
120	3.26	3.26	0	0	1.0	2.5	71.6	16.1	8.7
135	9.14 (neat)	0	4	0	0.22	95.5	3.2	1.1	...
165	9.14 (neat)	0	4	4	0.19	97.8	1.6	0.33	...
165	3.26	3.26	4	4	1.5	76.1	15.5	3.9	3.0
0	3.26	3.26	0	0	0	99.1	0.71	0.22	0
28					0	94.5	3.5	1.3	0.68
56					0.34	74.1	17.2	3.8	4.3
91					0.75	29.7	42.9	4.4	22.2
124					1.6	3.3	58.7	12.6	23.9
148					1.5	4.7	55.7	12.0	26.1

[a] Photocatalyst is [S]≥$SiCo(CO)_4$ (sample no. 3 of Table II); 0.045 g of this powder was suspended in 1.0 mL of the indicated solution and deoxygenated. Irradiation was at 25 °C using a Pyrex-filled 450-W Hg arc lamp under the same conditions for each sample. Analyses were by gas chromatography. All samples were stirred during the irradiation. On the time scale of these experiments no thermal reaction is detectable in the dark.

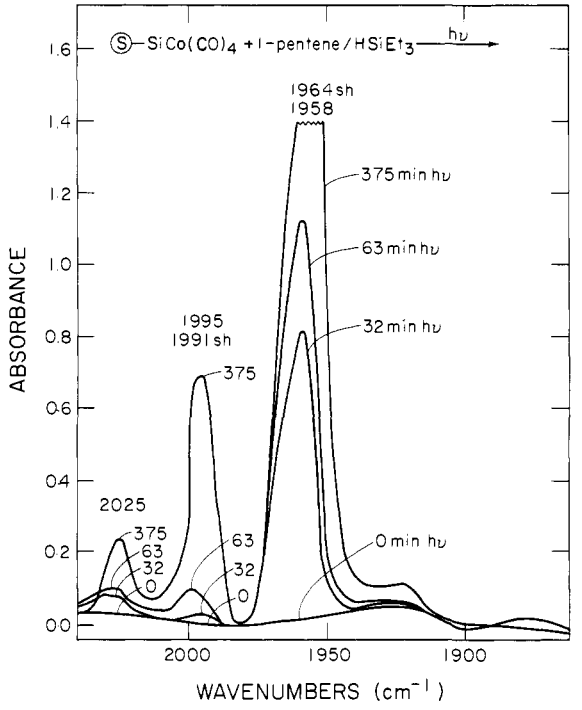

Figure 6. Infrared spectral changes in solution accompanying the irradiation of a derivatized alumina surface in the presence of 1-pentene/$HSiEt_3$. The solution products are the same as those observed when homogeneous $Et_3SiCo(CO)_4$ (photochemical) or $Co_2(CO)_8$ (thermal) is used as the cobalt source. The bands at 2025, 1995, and 1991 (sh) cm^{-1} are due to $Et_3SiCo(CO)_4$.

of 1-pentene leads to the generation of $Co_4(CO)_{12}$ in solution. Infrared analysis of the irradiated powder shows loss of $-Co(CO)_4$ groups and the growth of weak absorptions in the C–H stretching region that could be due to [S]≥Si(pentenyl). Photolysis of $Et_3SiCo(CO)_4$ in the presence of 1-pentene yields Et_3Si(pentenyl) as the only Si-containing product.[12] The irradiated powder also shows consumption of [S]≥SiH functionality. Apparently, the Si–H groups not originally reacted with $Co_2(CO)_8$ can react with photoreleased Co–carbonyl fragments and subsequently with 1-pentene to yield [S]≥Si(*n*-pentyl); that is, the residual [S]≥SiH reacts with the Co-carbonyl/1-pentene to hydrosilate the 1-pentene. Thus, reaction with alkene and [S]≥SiH/≥$SiCo(CO)_4$ can be induced photochemically. However, there is no accumulation of catalysis products in solution. Even alkene isomerization activity (1-pentene → *cis*- or *trans*-2-pentene) is nil.

Irradiation of [S]≥$SiCo(CO)_4$ in the presence of 1/1 mixtures of 1-pentene/Et_3SiH does result in catalytic chemistry. For example, near-UV irradiation of 0.045 g of [S]≥$SiCo(CO)_4$, sample no. 3 in Table II, in the presence of 0.39 M Et_3SiH/0.39 M 1-pentene in isooctane rapidly yields infrared detectable metal carbonyls in the supernatant solution. Initially, $Et_3SiCo(CO)_4$ is formed, and irradiation also yields infrared absorptions in the supernatant at 1960 and 1966 (sh) cm^{-1} that have been previously observed, but not unambiguously assigned,[12,15] in solutions initially containing $Co_2(CO)_8$/1-pentene/Et_3SiH. Gas chromatographic analysis of the solution after 48 min of irradiation shows the following composition (% based on initial 1-pentene concentration): pentane (4.2); 1-pentene (1.3); *trans*-2-pentene (46.3); *cis*-2-pentene (15.5); (*n*-pentyl)$SiEt_3$ (32.7). Thus, photocatalysis is effected (eq 8). On the time scale of this experiment there is

$$\text{1-pentene} + Et_3SiH \xrightarrow[\text{near-UV}]{\text{[S]}\geq SiCo(CO)_4} \textit{n}\text{-pentane, } \textit{cis}\text{-2-pentene, } \textit{trans}\text{-2-pentene, } (\textit{n}\text{-pentyl})SiEt_3 \quad (8)$$

no thermal catalysis. Further, Al_2O_3, Al_2O_3 treated only with $Co_2(CO)_8$, or Al_2O_3 treated only with $(EtO)_3SiH$ gives neither thermal nor photoinduced catalysis under the same conditions. Thus, the [S]≥$SiCo(CO)_4$ would appear to be a photochemical precursor to catalysis. In view of the photogeneration of $Et_3SiCo(CO)_4$ from [S]≥$SiCo(CO)_4$, eq 4–7, in the presence of Et_3SiH or in the presence of Et_3SiH/1-pentene, catalysis should result if for no other reason than $Et_3SiCo(CO)_4$ yields catalysis when irradiated in the Et_3SiH/1-pentene mixture.[12]

Irradiation of [S]≥$SiCo(CO)_4$ in the presence of neat 1/1 Et_3SiH/1-pentene results in catalytic chemistry. Data for a typical photocatalysis run are included in Table III. No dark reaction occurs on the time scale of this experiment. Infrared analysis of the [S]≥$SiCo(CO)_4$ shows >95% loss of $-Co(CO)_4$ from the Al_2O_3 surface at ~30-min irradiation time. Analysis of the solution shows the growth of the absorptions at ~1960 cm^{-1} found in thermal reactions of $Co_2(CO)_8$ with Et_3SiH/1-pentene[15] and photoreactions of $Et_3SiCo(CO)_4$ with Et_3SiH/1-pentene.[12] At longer irradiation times infrared bands for $Et_3SiCo(CO)_4$ become apparent and the 1960-cm^{-1} feature intensifies somewhat. After 375 min, there are no detectable Co–carbonyl fragments on the surface of the Al_2O_3. The mol % of Si–H in the Al_2O_3 decreases during the irradiation, likely reflecting the generation of [S]-≥Si(*n*-pentyl).

The main conclusion regarding catalysis from the irradiations of [S]≥$SiCo(CO)_4$ in the presence of Et_3SiH/1-pentene is that the bulk of the catalysis occurs from the photoreleased Co–carbonyl fragments. For example, in the particular run detailed in Table III, most (>95%) of the Co–carbonyl is in homogeneous solution after the ~30-min irradiation time. To provide additional confirmation of this conclusion, we irradiated 0.0759 g of [S]-≥$SiCo(CO)_4$ sample no. 3 in Table II, in 1 mL of neat Et_3SiH until ~80% (~80 min irradiation) of the $-Co(CO)_4$ was present in solution as $Et_3SiCo(CO)_4$. The supernatant was diluted with 1-pentene to bring the Et_3SiH/1-pentene to a 1/1 mole ratio. Irradiation of the $Et_3SiCo(CO)_4$/Et_3SiH/1-pentene gave photo-

Table IV. Photocatalysis of Neat 1:1 1-Pentene/$HSiEt_3$ Solutions by Various Preparations of [S]≻$SiCo(CO)_4$[a]

support	irrdn time, h	product distribution, %				
		n-pentane	1-pentene	*trans*-2-pentene	*cis*-2-pentene	Et_2Si(*n*-pentyl)
SiO_2 powder (low surface area; low coverage of $-Co(CO)_4$)	0	0.032	99.7	0	0.19	0
	4.25	0.96	28.9	60.8	5.4	4.0
	12	1.3	1.6	75.4	14.6	7.2
	69	1.9	0.94	48.0	1.5	45.7
	69 (dark)[b]	0.084	2.9	2.9	0.17	0.25
γ-Al_2O_3 pellets (sample no. 1 of Table II)	0	0.032	99.7	0	0.20	0
	4.25	0.030	99.8	0	0.12	0.061
	12	0.14	92.1	7.1	0.26	0.47
	24	2.6	4.4	77.6	10.6	4.8
	69	1.7	2.3	80.6	10.2	5.3
	69 (dark)[b]	0.11	99.1	0.78	0.034	0.067
Woelm Al_2O_3 (sample no. 7' of Table II)	0	0.029	99.8	0	0.12	0
	4.25	0.94	86.3	11.5	0.62	0.53
	24	2.6	16.5	69.1	8.7	3.0
	69	3.9	2.0	87.4	2.3	4.3
	69 (dark)[b]	0	99.9	0	0.14	0
γ-Al_2O_3 powder (sample no. 2 of Table II)	0	0.032	99.8	0	0.19	0
	4.25	0.63	80.9	16.6	0.83	1.1
	12	1.7	24.1	67.6	2.5	4.1
	69	2.4	1.6	86.0	1.0	9.0
	69 (dark)[b]	1.2	12.5	73.6	8.0	4.6
γ-Al_2O_3 powder (sample no. 3 of Table II)	0	0.031	99.7	0	0.19	0
	0.5	0.22	93.5	5.0	0.94	0.40
	1.0	0.64	64.0	29.2	3.4	2.8
	4.25	3.1	1.6	86.2	1.3	8.0
	64	13.0	0.14	9.6	1.9	74.5
	64 (dark)[b]	2.6	16.0	76.3	0.36	4.9

[a] 0.045 g of [S]≻$SiCo(CO)_4$ in 1 mL of degassed $HSiEt_3$/1-pentene irradiated at 355 nm at ~2×10^{-6} einstein/min at 25 °C. All solutions were stirred. [b] Dark denotes samples that were treated in parallel with other samples for the indicated time but were not exposed to light.

catalytic action with a rate and product distribution very similar to that when the [S]≻SiH/≻$SiCo(CO)_4$ phase was not removed. The catalytic products and their initial ratios accord well with previous findings in this laboratory from thermal catalysis using $Co_2(CO)_8$ or photocatalysis using $Et_3SiCo(CO)_4$.[12] Thus, we firmly conclude that photocatalytic action from [S]≻$SiCo(CO)_4$ results from reactive Co–carbonyl fragments released into homogeneous solution. The active species appears to be the same as that involved in $Co_2(CO)_8$ or $Et_3SiCo(CO)_4$ catalysis.

e. Photocatalysis Results under Variable Conditions. Photocatalysis of Et_3SiH/1-pentene mixtures has been carried out by using various preparations of [S]≻$SiCo(CO)_4$ and under variable conditions. Table IV details results for various preparations of [S]≻$SiCo(CO)_4$ where the major variable would appear to be the amount of $-Co(CO)_4$ actually added when 0.045 g/mL of [S]-≻$SiCo(CO)_4$ is added to the mixture. Note that the irradiation source (355 ± 20 nm, 2×10^{-6} einstein/min) for the experiments summarized in Table IV has lower intensity than for the Pyrex-filtered 450-W Hg arc used for the experiments summarized in Table III. Accordingly, the reaction times are longer. Variations in the activity of the [S]≻$SiCo(CO)_4$ system crudely parallel the expectations for rate of release of $-Co(CO)_4$. Higher coverages and large surface areas provide for a higher rate of appearance of active material in solution. All of the catalyst precursors yield the same Si-containing product, namely, Et_3Si(*n*-pentyl) and rather small amounts of pentane. In cases where there is significant dark reaction at 25 °C on the 69-h time scale we also find very rapid photocatalytic action. The thermal activity in the dark is attributable to a slow thermal process again involving loss of CO as the rate-limiting step. However, under all conditions the light-activated catalysis proceeds more rapidly even at the low light intensity. For the data given in Table III, where the 450-W Hg arc source was used, the dark thermal controls show little or no reaction on the time scale of the experiments summarized.

Table III includes data for reactions carried out in neat 1/1 Et_3SiH/1-pentene mixtures exposed to H_2 or H_2/CO mixtures. The data show that the product distribution under 4 psig of H_2 shifts markedly to higher yields of pentane. However, irradiation of [S]≻$SiCo(CO)_4$ in the presence of neat 1-pentane and 4 psig of H_2 yields little isomerization or hydrogenation. These results are consistent with our previous findings for photoactivation of alkene catalysis using Co–carbonyl species: H_2 as an oxidative addition substrate to create hydrides for isomerization or reduction does not seem to be effective.[20] The H_2/CO atmosphere suppresses the rate of catalysis even at the 4 psig of CO pressure used. The resulting product mixture contains no detectable hydroformylation products. The suppression of catalysis is associated with the capture of coordinatively unsaturated sites by the CO. The effects of H_2 and H_2/CO parallel those found earlier for photocatalysis of alkene reactions using Co–carbonyl species.[12,20]

The ability to functionalize [S]≻$SiCo(CO)_4$ by photosubstitution affords an opportunity to examine the photocatalytic activity of [S]≻$SiCo(CO)_3(P(OPh)_3)$. Irradiation of [S]≻$SiCo(CO)_4$ in the presence of $P(OPh)_3$ followed by decanting and washing yields a mixture of [S]≻$SiCo(CO)_3(P(OPh)_3)$ and [S]≻$SiCo(CO)_4$. Use of this mixture as a catalyst precursor compared to pure [S]-≻$SiCo(CO)_4$ under the same conditions yields an important difference in the catalytic products (Table V). The formation of at least two isomers of Et_3Si(pentenyl) accompanies the usual distribution of products. Such products have previously been found from the thermal and photocatalyzed reaction of Et_3SiH/1-pentene mixtures using $Fe(CO)_5$[21,22] and $M_3(CO)_{12}$ (M = Fe, Ru, Os).[23] Another difference in the product distribution is the lower initial trans/cis ratio of the 2-pentene isomers compared to the catalyst having no $P(OPh)_3$ present. Analysis of the [S]≻$SiCo(CO)_4$/≻$SiCo(CO)_3(P(OPh)_3)$ powder shows loss of Co–carbonyl species, again indicating that the catalysis occurs via photoreleased Co–carbonyl fragments. The very different product ratio with the $P(OPh)_3$ complex indicates that the actual catalyst is different than that for [S]≻$SiCo(CO)_4$. It is attractive to conclude that CO loss is again the primary photoreaction leaving $P(OPh)_3$ in

(20) Reichel, C. L.; Wrighton, M. S. *J. Am. Chem. Soc.* **1979**, *101*, 6769.
(21) Nesmeyanov, A. N.; Friedlina, R. K.; Chukovskaya, E. C.; Petrova, R. G.; Belyavksy, A. B. *Tetrahedron* **1961**, *17*, 61.
(22) Schroeder, M. A.; Wrighton, M. S. *J. Organomet. Chem.* **1977**, *128*, 345.
(23) Austin, R. G.; Paonessa, R. S.; Giordano, P. J.; Wrighton, M. S. *Adv. Chem. Ser.* **1978**, *No. 168*, 189.

Table V. Comparison of Catalytic Properties of [S]⩾$SiCo(CO)_4$ and [S]⩾$SiCo(CO)_3(P(OPh)_3)$[a]

attached catalyst	hν, min	product distribution, %						
		n-pentane	1-pentene	*trans*-2-pentene	*cis*-2-pentene	Et_3Si(*n*-pentyl)	isomers of Et_3Si(pentenyl)	
[S]⩾$SiCo(CO)_4$ (sample no. 2 of Table II)	0	0	100	0	0	0	0	0
	45	0.46	57.8	36.5	3.2	2.0	0	0
	60	0.68	25.9	63.7	7.9	1.8	0	0
	75	0.99	21.5	66.6	7.7	3.2	0	0
	250	1.6	3.4	77.6	12.3	5.1	0	0
	250 (dark)[b]	0	100	0	0	0	0	0
[S]⩾$SiCo(CO)_nL_{4-n}$	0	0	100	0	0	0	0	0
$n = 4$, 25.6%	30	0	98.9	0.40	0.19	0.28	0.028	0.17
$n = 3$, 74.4%	45	0.18	95.7	2.7	0.15	0.93	0.085	0.31
$L = P(OPh)_3$	75	0.42	83.1	10.1	0.92	4.3	0.39	0.76
(from sample no. 2 of	278	2.3	1.9	63.1	19.9	9.5	1.3	1.9
Table II by photosubstitution)	278 (dark)[b]	0	100	0	0	0	0	0

[a] 0.045 g of [S]⩾$SiCo(CO)_nL_{4-n}$ in degassed 1.0 mL of 1/1 Et_3SiH/1-pentene solution irradiated at 25 °C through Pyrex by using a 450-W Hg arc lamp. Solutions were analyzed by gas chromatography to determine composition. All samples were stirred during irradiation. [b] Dark denotes samples that were treated in parallel with other samples for the indicated time but were not exposed to light.

Table VI. Comparison of Catalytic Activity of [S]⩾$SiCo(CO)_4$ and $Co_2(CO)_8$[a]

catalyst precursor	substrates	time, min (Δ or hν)	% conversion[b]	product[c]	turnover rate,[d] h^{-1}
$Co_2(CO)_8$ (0.002 M)	1-pentene/$HSiEt_3$ (3.26 M/3.26 M)	14 (Δ)	28.4	2-pentenes	1000
		24 (Δ)	54.4	2-pentenes	1100
		54 (Δ)	82.0	2-pentenes	750
		179 (Δ)	>85	2-pentenes	equilibrium attained[e]
$Co_2(CO)_8$ (0.002 M)	1-pentene/$HSiEt_3$ (3.26 M/3.26 M)	96 (Δ)	12.3	(*n*-pentyl)$SiEt_3$	125
		237 (Δ)	15.5	(*n*-pentyl)$SiEt_3$	60
		495 (Δ)	16.0	(*n*-pentyl)$SiEt_3$	32
[S]⩾$SiCo(CO)_4$ (0.004 M)[f]	1-pentene/$HSiEt_3$ (3.26 M/3.26 M)	56 (hν)	21.0	2-pentenes	180
			4.0	(*n*-pentyl)$SiEt_3$	35
		91 (hν)	47.3	2-pentenes	250
			22.2	(*n*-pentyl)$SiEt_3$	120
		124 (hν)	71.3	2-pentenes	equilibrium attained[e]
			23.9	(*n*-pentyl)$SiEt_3$	90

[a] Samples of [S]⩾$SiCo(CO)_4$ or $Co_2(CO)_8$ in deoxygenated 3.26 M/3.26 M 1-pentene/$HSiEt_3$ were reacted at 20 °C in the dark ($Co_2(CO)_8$) or under illumination from a 450-W Hanovia Hg arc ([S]–$SiCo(CO)_4$). [b] % Conversion to indicated products based on 1-pentene. [c] The products from catalysts are the 2-pentenes and (*n*-pentyl)$SiEt_3$; cf. Tables III–V. [d] Turnover rate is the number of product molecules formed per hour per Co atom initially added as either $Co_2(CO)_8$ or [S]⩾$SiCo(CO)_4$. [e] At this point the linear pentenes are close to the thermodynamic ratio. [f] This concentration is the total effective –$Co(CO)_4$ concentration assuming the –$Co(CO)_4$ to be completely efficiently released. The sample used is no. 3 of Table II and data are from Table III.

the coordination sphere to influence product ratios by steric and electronic effects. The catalytic activity appears to be somewhat lower than for the unsubstituted [S]⩾$SiCo(CO)_4$. This is very likely due to lower quantum yields for the primary process of CO loss from the $P(OPh)_3$ complex.

f. Comparison of Catalytic Activity of [S]⩾$SiCo(CO)_4$ with $Co_2(CO)_8$. Photoexcitation of [Si]⩾$SiCo(CO)_4$ in the presence of 1-pentene/$HSiEt_3$ mixtures apparently yields the same catalyst species that results from the irradiation of $Et_3SiCo(CO)_4$.[12] Further, we have previously concluded that the irradiation of $Et_3SiCo(CO)_4$ leads to the active species formed thermally from $Co_2(CO)_8$.[12,15] Thus, comparison of the catalytic activity of $Co_2(CO)_8$ and [S]⩾$SiCo(CO)_4$ is appropriate. We have examined the initial thermal activity of $Co_2(CO)_8$ at 20 °C for isomerization and hydrosilation of 1-pentene under the same conditions where we can photoactivate the [S]⩾$SiCo(CO)_4$ system. Data in Table VI are representative of the activity of the two different precursor systems. In both systems the isomerization products are formed at a faster rate than the hydrosilation products and it would appear that the rate of formation of hydrosilation products declines as the 1-pentene is converted to the 2-pentenes. This is reasonable, since it is likely that the hydrosilation of 1-pentene is more rapid than the same reaction of the internal isomers. The interesting finding is that the photoactivated system is in fact quite similar in turnover rate to the $Co_2(CO)_8$ thermal system. Further, since the observed rate of product formation depends on excitation rate (light intensity), the turnover rate for the photoactivated system could be even higher at higher light intensity. In both systems it would appear that the isomerization turnover number is similar; we find that the number of product molecules formed is generally limited by substrate concentration not catalyst lifetime. For hydrosilation, we have already demonstrated that illumination of $Et_3SiCo(CO)_4$ allows more turnovers for (*n*-pentyl)$SiEt_3$ formation, since the $Co_2(CO)_8$ thermal system ultimately ceases activity due to formation of $Et_3SiCo(CO)_4$ that is not thermally active.

Irradiation of species such as $R_3SiCo(CO)_4$ does result in persistent thermal activity in the dark at 20 °C. However, the activity is relatively low and short-lived. For example, a flash excitation of $Ph_3SiCo(CO)_4$ leads to ~50% dark isomerization of 1 M 1-pentene in the presence of 1 M $HSiEt_3$ during a 4-h period. Continuous irradiation leads to nearly complete equilibration of the linear pentenes under the same conditions in <4 h. Thus, considerable activity can persist in the dark, but irradiation accelerates the catalytic rate even further.

Summary

The data adequately demonstrate that –$Co(CO)_4$ anchored to oxide surfaces via reaction of $Co_2(CO)_8$ with [S]⩾SiH exhibits photochemistry that parallels that for solution $R_3SiCo(CO)_4$ analogues. The photoinduced loss of CO is the principal result of photoexcitation of either $R_3SiCo(CO)_4$ in solution[12] or [S]⩾$SiCo(CO)_4$ suspended in solutions. In neither case do we find evidence for prompt scission of the Co–Si bond, but in each case reaction with R_3SiH or alkenes leads to chemically efficient loss of the original Co–Si bond. For [S]⩾$SiCo(CO)_4$ this means that the Co–carbonyl species does not remain anchored to the surface. Thus, with this system we have not achieved the capability of "matrix-isolating" photogenerated, coordinatively unsaturated

intermediates. However, the [S]>$SiCo(CO)_4$ system as a catalyst precursor is easily handled and is less sensitive to O_2 than is the solution species $Et_3SiCo(CO)_4$. The concept of releasing a catalyst photochemically at a rate controlled by light intensity is one that could be exploited, in principle, in catalytic reactions.

Acknowledgment. We thank the Office of Naval Research for partial support of this research. Support from the Dow Chemical Co. is also gratefully acknowledged. Support for the Fourier transform infrared spectrometer was supplied by the National Institutes of Health, Grant No. GM 27551.

Synthetic Applications of Conjugated Azocarbinols. Radical Chain Hydrophenylation and Hydrocyclohexenylation of Haloethenes†

Yau-Min Chang, Ralph Profetto, and John Warkentin*

Contribution from the Department of Chemistry, McMaster University, Hamilton, Ontario, Canada L8S 4M1. *Received April 13, 1981*

Abstract: 2-(Phenylazo)-2-propanol (**5**) and (phenylazo)diphenylmethanol (**6**) decompose in solution by processes involving phenyl radicals. Similarly, 1-(1-azocyclohexenyl)cyclohexanol (**7**) decomposes in solution to generate the 1-cyclohexenyl radical. Evidence for radical intermediates includes the formation of chlorobenzene and 1-chlorocyclohexene, respectively, from decomposition of **5** (or **6**) and **7** in CCl_4. Evidence for induced, chain decomposition by radical abstraction of hydroxyl hydrogen, in concert with breaking of at least one C–N bond of the azo function, includes faster decomposition in CCl_4 than in benzene, acceleration of decomposition in CCl_4 by thiophenol, and acceleration of decomposition in benzene by trityl radicals. That decomposition mechanism is supported also by the finding that methyl ethers and acetate esters of the azoalcohols decompose much more slowly than the alcohols themselves. Phenyl radicals from either **5** or **6**, and 1-cyclohexenyl radicals from **7**, can be trapped with some alkenes by addition. Such radical adducts subsequently pick up a hydrogen atom, presumably by abstracting from the hydroxyl group of the azocarbinol in concert with C–N bond breaking. The overall processes, then, are hydrophenylation of alkenes with **5** or **6** and hydro-1-cyclohexenylation of alkenes with **7** by a radical chain mechanism. The processes are of preparative value only in cases of alkene substrates which are neither highly polymerizable nor prone to radical attack on allylic substituents. Several highly halogenated compounds prepared by treatment of haloethenes with **6** or **7** are reported. The reaction between **5** and benzaldehyde, to form acetone and 1-benzoyl-2-phenylhydrazine, was found to be second order overall, first order in **5** and first order in benzaldehyde between 0.4 M and neat benzaldehyde. This result does not appear to be compatible with a mechanism involving decomposition of **5** to acetone and phenyldiazene, with subsequent reaction of the latter with benzaldehyde.

Recently we reported some free radical chemistry of compounds having the α-hydroxyalkyl azo function, HO—C—N=N.[1-4] Such molecules, **1** and **2**, for example, appear to undergo radical chain, induced decomposition by attack at hydroxyl hydrogen (eq 1 and 2).[3] It was possible to make use of such compounds as reagents for radical chain hydroalkylation of alkenes and alkynes (eq 3).[4]

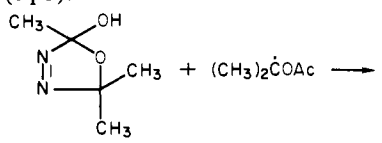

1

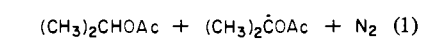

(1)

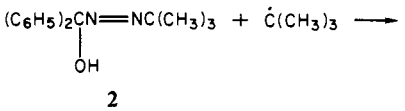

2

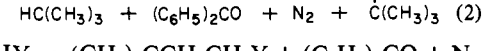

(2)

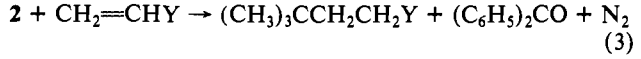

(3)

It was interesting to ask whether the chain-transfer ability of the azocarbinol systems would be sufficiently high to permit their use for radical chain hydrophenylation (e.g. with **6**) and hydro-1-alkenylation (e.g., with **7**) of olefinic substrates. We report the first examples (eq 4 and 5) of those synthetic applications in this paper.

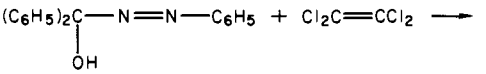

6

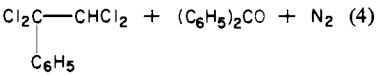

(4)

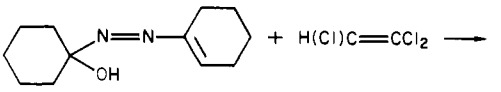

7

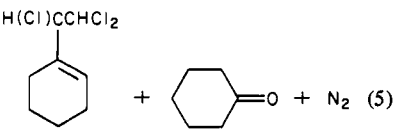

(5)

† Dedicated to Dr. George S. Hammond on the occasion of his 60th birthday.

(1) α-Hydroxyalkyl azo compounds were first reported by Schmitz and co-workers[2a,b] and subsequently by Hünlg's group.[2c-f] They have also been called α-hydroxyalkyldiazenes, semiaminals of diimide, and, by us, azocarbinols. We continue to use the latter, simple but not rigorous, name for the class.

(2) (a) Schmitz, E.; Ohme, R.; Schramm, S. *Angew. Chem., Int. Ed. Engl.* **1963**, *2*, 157. (b) Schmitz, E.; Ohme, R.; Schramm, S. *Justus Liebigs Ann. Chem.* **1967**, *702*, 131. (c) Hünig, S.; Cramer, J. *Angew. Chem., Int. Ed. Engl.* **1968**, *7*, 943. (d) Hünig, S.; Büttner, G. *Ibid.* **1969**, *8*, 451. (e) Büttner, G.; Hünig, S. *Chem. Ber.* **1971**, *104*, 1088. (f) Büttner, G.; Cramer, J.; Geldern, L.; Hünig, S. *Ibid.* **1971**, *104*, 1118.

0002-7863/81/1503-7189$01.25/0